Proceedings of Global Power and Propulsion Society
ISSN-Nr: 2504-4400
GPPS Xi'an21
18th – 20th October, 2021
www.gpps.global

GPPS-TC-2021-0041

Research of laws and prediction of axial-flow compressor characteristics based on data driven

Tantao Liu
School of Power and Energy, Northwestern Polytechnical University
liutantao@mail.nwpu.edu.cn
Xi'an, Shaanxi, China

Limin Gao
School of Power and Energy, Northwestern Polytechnical University
gaolm@nwpu.edu.cn
Xi'an, Shaanxi, China

Xudong Feng
Aero Engine Corporation of China, Sichuan Gas Turbine Establishment
363166446@qq.com
Mianyang, Sichuan, China

ABSTRACT

The performance maps of axial-flow compressors are critical to the operation and design of gas turbines. To explore the inherent laws of axial-flow compressors performance map, more than 50 axial-flow compressors' maps were studied based on data analysis and thermodynamic principles. By introducing a variety of thermodynamic and mechanical parameters into the performance lines, relations between different quantities of compressors were built from three aspects which are peak efficiency lines, near-surged zones and near-choked zones. The relations between compressor characteristic parameters and design performance indexes were found and the prediction algorithm was developed to predict performance of compressors based on design performance indexes and performance parameters. It shows that there are linear relations between thermodynamics parameters within working speed range. The performance parameters of compressors are obvious relative with design total pressure ratio and little relative with design efficiency. The prediction algorithm can predict the performance map of compressors well just relied on design performance indexes and performance parameters without blades geometry information.

1.INTRODUCTION

Axial-flow compressors are important components of gas turbines, which are widely used in aviation propulsion, ship power and power station to compress the air. The compressor performance map (Dixon, et al. 2014) is the illustration of compressor aerodynamic characteristics in the whole operating range and it is also the basis of the actual operation for aero-engines or gas turbines. It is generally expressed as the relations between the total pressure ratio, efficiency and mass flow, speed.

During monitoring the operating of a gas turbine and initial design of an aircraft engine, the characteristics map of the compressor is needed. At present, there are a variety of studies on compressor characteristics. Most of these investigations focus on extending the map to the low speed zone or off-design zone, interpolation between different speed lines and the performance prediction based on artificial intelligent.

Kurzke (1996, 2005, 2011) introduced β-lines as an auxiliary coordinate to solve the problem of fitting vertical speed lines, proposed a MAP format to describe turbomachinery performance map which had been applied by software GasTurb and developed an algorithm to predict low speed performance of compressors after analysing the laws hidden in the compressor maps. Based on incompressible flow theory and compressible modified method, Wang et al. (2006) developed a component characteristic model of turbofan engine under idle speed, which can calculate the windmill characteristics of gas engines reasonably.

Tsoutsanis et al. (2012a, 2012b, 2015) used the elliptic curve and the genetic optimization algorithm to describe the compressor maps and determined the fitting coefficient according to the test data and optimization algorithm to predict and diagnose the gas turbine operation. Zagorowska et al. (2017) used Chebyshev polynomials to approximate the characteristics of centrifugal compressor, which shows that this method captures all the important aspects of compressors. Fei et al. (2016) proposed a feed-forward BP neural network with a Gaussian kernel function to extrapolate and interpolate compressor performance maps. Li et al. (2018) used two kinds of partial least squares models to interpolate and extrapolate the compressor maps. Mikhailova et al. (2014, 2016) considered the compressor operation process and proposed K_1 and K_2 parameters. The relationship between the two parameters and flow coefficient, circumferential Mach number was proposed and a prediction method of the off-design performance of the compressor was developed.

Above all, it can be seen that most studies about compressor characteristics focus on a single compressor. Few research compares different compressors and explores the relations between compressor maps and their design performance indexes such as the design total pressure ratio and the design efficiency. During aero engine preliminary design, the approximate compressor characteristics map is needed for the overall performance calculation of the aero engine. However, in most cases no blade geometry data can be provided during this period. So, it is necessary to provide a prediction algorithm to predict the performance based on design parameters.

In this paper, there are two purposes: the first one is to discover the inherent laws hidden in characteristic maps of compressors and the second is to develop an algorithm to predict the performance map of the compressors just base on design performance indexes. We analysed more than 50 compressors' characteristics maps based on data analysis and thermodynamics principles to acquire the inherent laws and found the relation between characteristics parameters and design performance indexes. According to above analysis, the compressor performance prediction algorithm relying on only performance at the design point was developed. Only simple algebraic calculation without iterations is needed, so the algorithm can run very fast. As no blade geometry data are needed, this algorithm is appropriate for overall performance calculation during preliminary design of gas turbines. It can also provide a reference for design and operating of compressors. It also helps to evaluate the performance of different compressors by comparing the performance coefficients.

The structure of this paper is as follows: The pre-processing of compressors' characteristics data is introduced in Section 2. Section 3 shows the analysis of efficiency peak points. Section 4 and Section 5 provide the study of near-choked zones and near-surged zones respectively. Base on above research, in Section 6 the prediction algorithm of compressor characteristic map is developed and the prediction results are shown. Concluding remarks are given in Section 7.

2.PREPROCESSING OF COMPRESSORS' CHARACTERISTICS DATA

Usually, the characteristics formulations can be represented by followings:

$$(\pi,\eta) = f(m_{\mathrm{cor}}, n_{\mathrm{cor}}) \tag{1}$$

Where π and η represents the total pressure ratio and isentropic efficiency respectively and m_{cor}, n_{cor} are corrected massflow and rotational speed. In general, the characteristic data obtained from compressor tests or manufactories are mostly in the form of line graphs expressing relations between total pressure ratio, efficiency and the massflow rate at each rotational speed.

The data set used by this paper includes axial-flow rotors, single stage compressors and multi-stages compressors designed for power plants, ships and aeroplanes. All the data come from NASA technical reports, papers of journals and academic conferences from 1970s to nowadays, including most of the published compressor characteristic maps. The design pressure ratios range from 1.3 to 22. It can be considered that the data set has a wide range of representativeness. As the data comes from a variety of literatures, the dimensions of the same physical quantity may be different. To further mining the laws in the data conveniently, the design point corrected massflow and corrected speed are used to normalize the corrected flow m and corrected speed n. If no otherwise specified, all the massflow and speed mentioned below are normalized quantities. Then the characteristics equations become

$$(\pi,\eta) = f(m,n) \tag{2}$$

The design point here is defined as the position in the characteristics map where the efficiency reaches maximum at the design speed. As the massflow and the efficiency had been normalized, at the design point, $n=n_{\mathrm{D}}=1$， $m=m_{\mathrm{D}}=1$. For most gas turbine and aero-engine, the working speed range is about 0.7 to 1.

3. CHARACTERISTIC OF PEAK EFFICIENCY POINTS

Agrawal (1981) found that in similar conditions, the speed, massflow and specific work have the following relations

$$\frac{m}{m_{\mathrm{r}}} = K_m \frac{n}{n_{\mathrm{r}}} \tag{3}$$

$$\frac{\Delta h^*}{\Delta h_{\mathrm{r}}^*} = K_h \left(\frac{n}{n_{\mathrm{r}}}\right)^2 \tag{4}$$

where the subscript r means the reference point, Δh^* represents specific work and K_m, K_h are empirical coefficients. However, the empirical coefficients make Eq. (3) and Eq. (4) be applied inconveniently. To eliminate the empirical coefficients, we can apply Eq. (3) and Eq. (4) only at peak efficiency points and let the reference point locate on the design point and make the exponents variable. Then Eq. (3) turns to be

$$\ln\left[\frac{m_{\mathrm{p}}(n)}{m_{\mathrm{d}}}\right] = E_m \ln\left(\frac{n}{n_{\mathrm{d}}}\right) + C_m \tag{5}$$

where subscript p represents peak efficiency points, E_m is the variable exponent and $C_m=\ln(K_m)$. When $n=n_{\mathrm{d}}=1$， $m_p(n)=m_{\mathrm{d}}=1$, then $C_{\mathrm{m}}=0$, namely $K_m=1$ when we choose the design point to be the reference point. So (5) can be further simplified as

$$\ln\left[m_{\mathrm{p}}(n)\right]=E_m\ln(n) \tag{6}$$

The logarithm relation of two compressors has been illustrated in Fig.1 and the linear fitting of peak efficiency points have been shown by dash lines. The red dots mean the peak efficiency points. It can be seen that the slopes (E_m) are different for the two compressors.

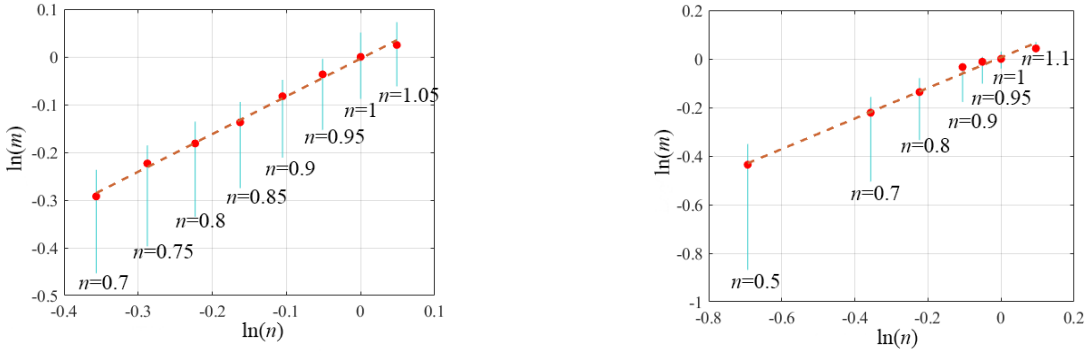

(a) A fan (b) A single rotor

Figure 1 Logarithm relation between massflow and speed at peak efficiency points (red dots)

To evaluate the accuracy of the linear fitting, Fig. 2 illustrates the Mean Squared Errors (MSE) distributions with different speed ranges and compressors. The design total pressure ratios are used to represent different compressors. Within the working speed range where n=0.7~1, the fitting errors are quite small, however, they increase obviously when the speed range is larger. The reasons may be that out of the working speed range, the flow in compressors is different as the shockwave is stronger and flow is seriously choked when the speed is high, while the air in compressors is nearly incompressible when the speed is low. For a few compressors, the MSE of different speed ranges keep the same, because only data of working speed are available for these compressors. The MSE of multi-stage compressors with high total pressure ratios is generally higher than that of low-pressure ratio compressor as for multi-stage compressors and the reason should be that the mass flow matching problem and other complex factors make a difference.

To investigate the relation between coefficient E_m and design performance indexes, Fig.3 illustrates the distribution of E_m and π_{d} of all the compressors which shows that the approximate linear relation between E_m and π_{d} conforms to

$$E_m(\pi_{\mathrm{d}})=0.19\pi_{\mathrm{d}}+0.75 \tag{7}$$

The left bottom zone which has been enlarged shows most points are near the fitting line and a small part of points are scattered. The reason for the dispersion is that the characteristic data come from a variety of literatures and some of them are special designed such as silent fans which show a completely different characteristics with others. In order to ensure the integrity, the special data sets are no deleted. For single stage or single rotor (π_{d}<2), E_m≈1, which conforms with Eq. (3). In the view of physics, E_m can represent the flow mass increasing rate with speed the along peak efficiency line. For high pressure ratio compressors, the greater E_m means that mass flow will change significantly when the speed change slightly as these compressors have strong bleeding ability. By the way, no obvious relation is found between E_m and the design efficiency η_{d}, so, for brevity, the illustration is not given.

The same method is applied to build the relations between specific work $\Delta h^*_{\mathrm{p}}(n)$ and total pressure ratio $\pi_{\mathrm{p}}(n)$:

$$\ln\left[\Delta h^*_{\mathrm{p}}(n)/\Delta h^*_{\mathrm{d}}\right]=E_h\ln(n) \tag{8}$$

$$\ln\left[\pi_{\mathrm{p}}(n)/\pi_{\mathrm{d}}\right]=E_\pi\ln(n) \tag{9}$$

where E_h, E_π are exponent coefficients of normalized specific work and normalized total pressure ratio respectively. The MSE of different speed ranges are shown in Fig. 4. Just like Fig. 2, the MSE in working speed range is least and the MSE increases sharply when the range is enlarged. Fig. 5 and Fig. 6 illustrate the distributions of E_h, E_π with π_{d} respectively, which show that E_h has no tendency to vary with π_{d} and there is a logarithmic relation between E_π and π_{d} that approximately corresponds with:

$$E_\pi(\pi_{\mathrm{d}})=0.65+1.22\ln(\pi_{\mathrm{d}}+0.50) \tag{10}$$

For low total pressure ratio compressors, the data points just locate almost on the fitting line, while for high π_{d} compressors, the corresponding points scattered near the fitting line. To further analyse E_h, the statistical density of E_h is presented in Figure 7, which shows E_h of most compressors distribute in the zone 2.29±0.56×2 and 2.29 and 0.56 are the mean and the standard variance respectively. It has been checked that the distribution of E_h is not normal distribution. In Eq. (4), the exponent is 2, however, for peak lines of most compressors, the exponent E_h is silently greater than 2. From the viewpoint of physics, both E_h and E_π or Δh^* and π can represent the energy imposed by a turbomachinery. The distinction is that Δh^* is the total energy including total pressure loss and the π only represents the isentropic part of the total energy added by blades.

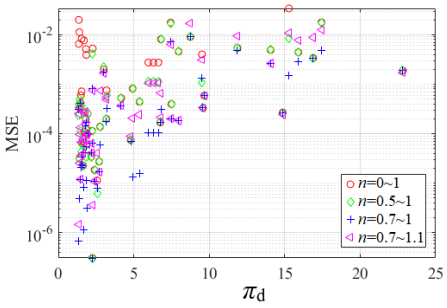

Figure 2 MSE of different speed range

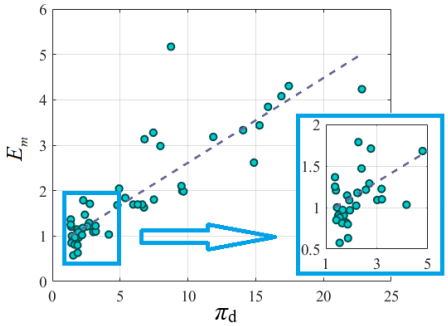

Figure 3 Distributions of E_m and π_d

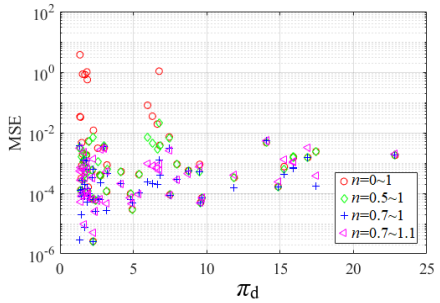

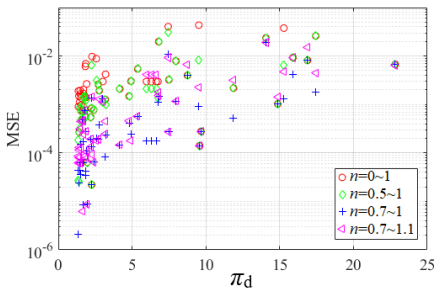

Figure 4 MSE of Eq.(8) (left) and Eq.(9) (right)

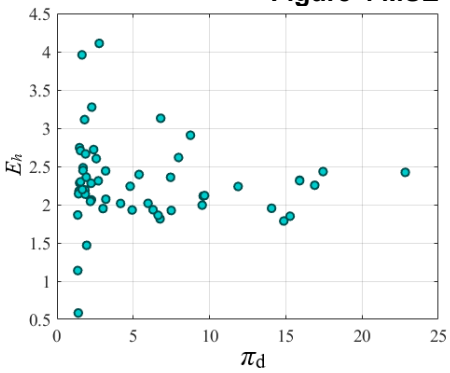

Figure 5 Distributions of E_h and π_d

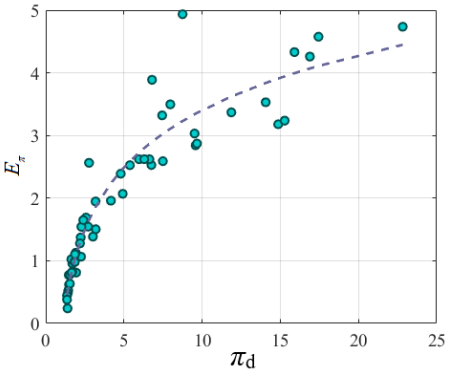

Figure 6 Distributions of E_π and π_d

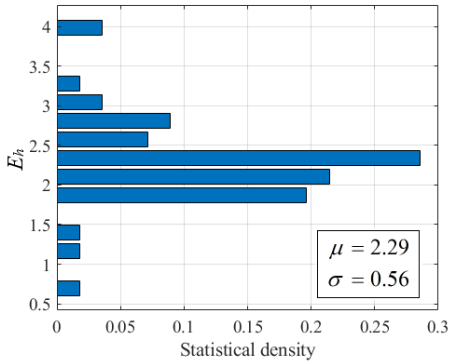

Fig 7. Statistical density distribution of E_h

4. INVESTIGATION OF NEAR-CHOKED ZONE

When the compressor is running on a constant speed with a decreasing back pressure, mass flow increases until it reaches the maximum, namely, the flow duct is choked. On the choking condition, the mass flow will be unchanged even if the back pressure continue to decrease. At this time, the characteristic lines are vertical on the performance map, which means that the same mass flow corresponds to a lot of working points. So, mass flow is no more suitable to be an independent variable. However, total pressure ratio which can follow the change of the back pressure can take the place of mass flow.

As we have already acquired the peak efficiency points and one purpose is to predict the characteristic, we hope to extend the characteristic from peak efficiency points. As there are two relations (m with π and m with η) in compressor

characteristic map, at least two independent equations are needed. After a lot of comparison, we find the two correlations in the near-choked zone.

The first one is the relation between the torque T and the total pressure ratio, which is shown in Figure 7 and the formulation is

$$\frac{T-T_{\mathrm{p}}}{T_{\mathrm{d}}}=k_{T-\pi}\left(\frac{\pi-\pi_{\mathrm{p}}}{\pi_{\mathrm{d}}}\right) \tag{11}$$

where the slope $k_{T-\pi}$ changes slightly with speed and varies with compressors of different design total pressure ratio, just shown in Fig. 8. In the second one, a new coefficient G which references Mikhailova's (2014) K_2 is proposed. It is defined by:

$$G=\frac{\Delta h_{\mathrm{s}}^{*}}{c_p T_1^{*} n^2}-\frac{m}{m_{\mathrm{p}}}\frac{\Delta h_{\mathrm{s,p}}^{*}}{c_p T_1^{*} n^2} \tag{12}$$

where the subscript p means the peak efficiency point at the same speed expect c_p which represents specific heat at constant pressure and T_1^{*} is the inlet total temperature. The relation between G and π is illustrated in Fig. 10 and can be formulated as:

$$G=k_{G-\pi}(\pi-\pi_{\mathrm{p}})/\pi_{\mathrm{d}} \tag{13}$$

where the slope $k_{G-\pi}$ is the function of speed n and π_{d}, namely, $k_{G-\pi}=k_{G-\pi}(n,\pi_{\mathrm{d}})$ shown in Figure 11 in which the numbers near the lines are corresponding π_{d} and for concise only 7 curves are plotted. This relation can be expressed by a response surface by Kriging surrogate model.

The lines emitted from peak efficiency points to choked points are straight in Figure 8 and Figure 10. So, the characteristics can be extrapolated from peak efficiency points.

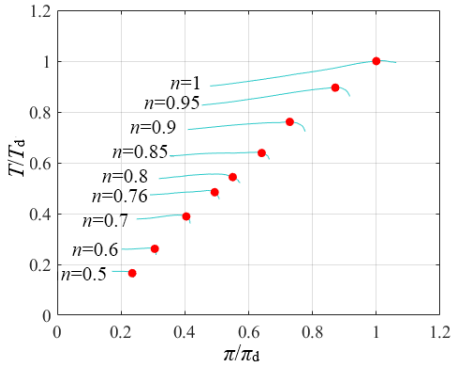

Fig 8. Relative toque and relative total pressure ratio of compressors

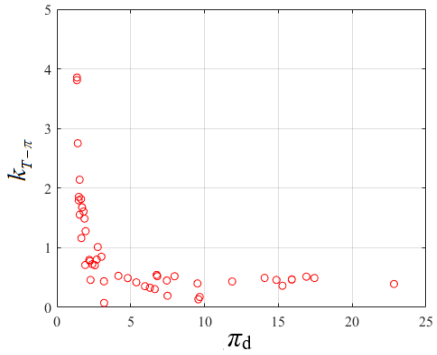

Figure 9. Distribution of slope $k_{T-\pi}$ with π_{D}

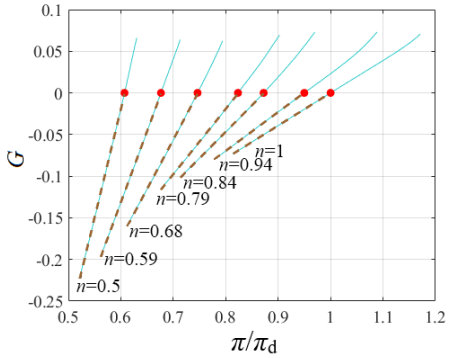

Figure 10. Relation between G and π_{d} with different speed

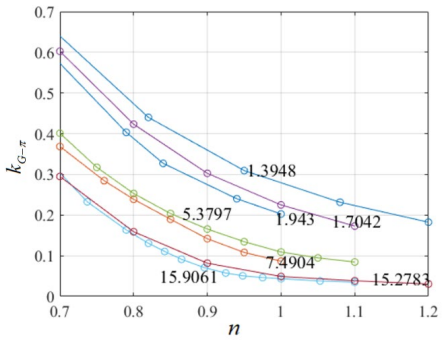

Figure 11. Relationship between π_{D}, n and $k_{G-\pi}$

5. INVESTIGATION OF NEAR-SURGED ZONE

In this section, the same method with previous section is adopted. For concise, only correlation expressions are listed:

$$\frac{\Delta h^{*}-\Delta h_{\mathrm{p}}^{*}}{\Delta h_{\mathrm{d}}}=k_{h-m}\left(\frac{m}{\pi}-\frac{m_{\mathrm{p}}}{\pi_{\mathrm{p}}}\right) \tag{14}$$

$$\frac{T/m^2 - T_p/m_p^2}{T_d/m_d^2} = k_{Tmm}\left(m - m_p\right) \tag{15}$$

where the slope coefficients conform with:

$$k_{h-m} = k_{h-m}(n, \pi_d) \tag{16}$$

$$k_{Tmm} = k_{Tmm}(n, \pi_d) \tag{17}$$

For a particular compressor, the two slope coefficients are nearly the same in working speed range. Again, the slopes can be expressed by response surfaces among different compressors.

6.PREDICTION OF COMPRESSORS' CHARACTERISTICS

The input parameters for the prediction include the design performance indexes (π_d and η_d) and three performance coefficients (E_m, E_π and E_h) which have been mentioned in Section 3. It is worth noting that Eq. (7) and (10) have proposed the approximate relation between E_m, E_π and π_d, however, the expressions are just a guide, not a straitjacket. If the aim of prediction is just a rough estimation, Eq. (7), (10) and E_h=2.29 can be adopted. In fact, different compressors with the same π_d and η_d may have different characteristics and the three coefficients are used to describe the difference. If a specific compressor performance is predicted, the three coefficients must reference similar compressors, which means the coefficients will float around previous recommend equations and value.

The first step: From Eq. (6), (8) and (9), considering the basic principles of turbomachinery, it can be deduced that:

$$m_p(n) = \exp[E_m \ln(n)] \tag{18}$$

$$\pi_p(n) = \pi_d \exp[E_\pi \ln(n)] \tag{19}$$

$$\eta_p(n) = \frac{\pi_p(n)^{(\gamma-1)/\gamma} - 1}{\left[\pi_d^{(\gamma-1)/\gamma} - 1\right]\exp\left[E_h \ln(n)\right]}\eta_d \tag{20}$$

With Eq. (18), (19) and (20), the characteristic points along the peak efficiency line are acquired in working speed range.

The second step is to extend characteristics from peak efficiency points to the near-choked zone and the near-surged zone. In the near-choked zone, total pressure ratio π is the independent variable and based on Eq.(11) and (13) and the definitions of torque and isentropic specific work, the mass flow and efficiency can be expressed as:

$$m(\pi) = m_p\left[\frac{\pi^{(\gamma-1)/\gamma} - 1 - n^2 k_G(\pi - \pi_p)/\pi_d}{\pi_p^{(\gamma-1)/\gamma} - 1}\right] \tag{21}$$

$$\eta(\pi) = \frac{\left(\pi_d^{(\gamma-1)/\gamma} - 1\right)m(\pi)}{n\left[k_{T-\pi}\dfrac{\left(\pi - \pi_p\right)}{\pi_d}\dfrac{\left(\pi^{(\gamma-1)/\gamma} - 1\right)}{\eta_d} + h_p\dfrac{m_p}{n}\right]} \tag{22}$$

where

$$h_p = \frac{\pi_p^{(\gamma-1)/\gamma} - 1}{\eta_p} \tag{23}$$

In the choked zone mass flow increases to the maximum monotonously, however, in Eq. (10), the $m(\pi)$ may not be monotonous with π. So, the monotonicity correction is needed to guarantee that the mass flow will not decrease once the maximum is reached and the $m(\pi)$ in Eq. (22) should be the corrected one.

In the near-surged zone, m is selected to be the independent variable, according to Eq. (14) and (15), mass flow and efficiency can be obtained by:

$$\pi(m) = \frac{m}{\dfrac{\Delta h^* - \Delta h^*_p}{\Delta h^*_d k_{h-m}} + \dfrac{m_p}{\pi_p}} \tag{24}$$

$$\eta(m) = \frac{\left(\pi^{(\gamma-1)/\gamma} - 1\right)}{\dfrac{\left(\pi_d^{(\gamma-1)/\gamma} - 1\right)}{\eta_d}k_{h-m}\left(\dfrac{m}{\pi} - \dfrac{m_p}{\pi_p}\right) + h_p} \tag{25}$$

where

$$\Delta h^* = \left[\Delta h^*_d k_{Tmm}(m - m_p) + \frac{\Delta h^*_p}{n_p m_p}\right]nm \tag{26}$$

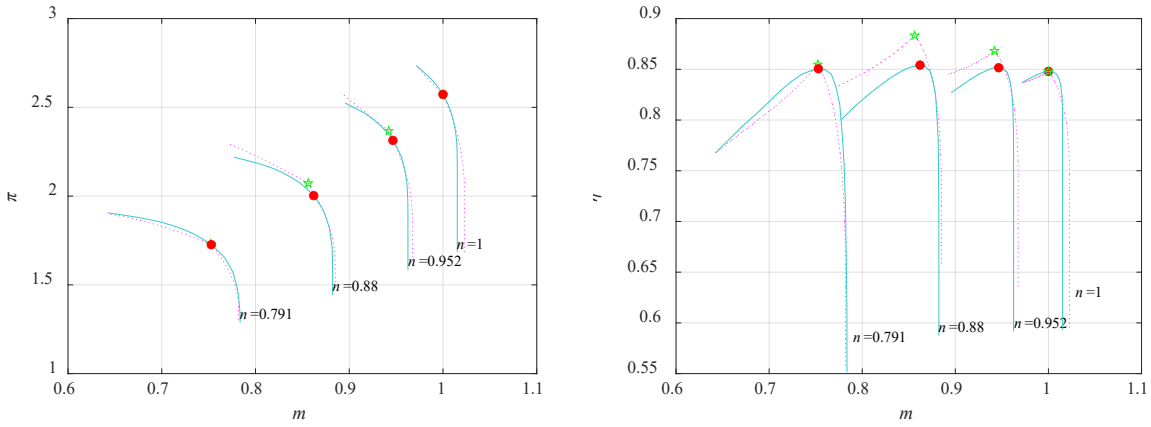

(a) Characteristics prediction of a booster

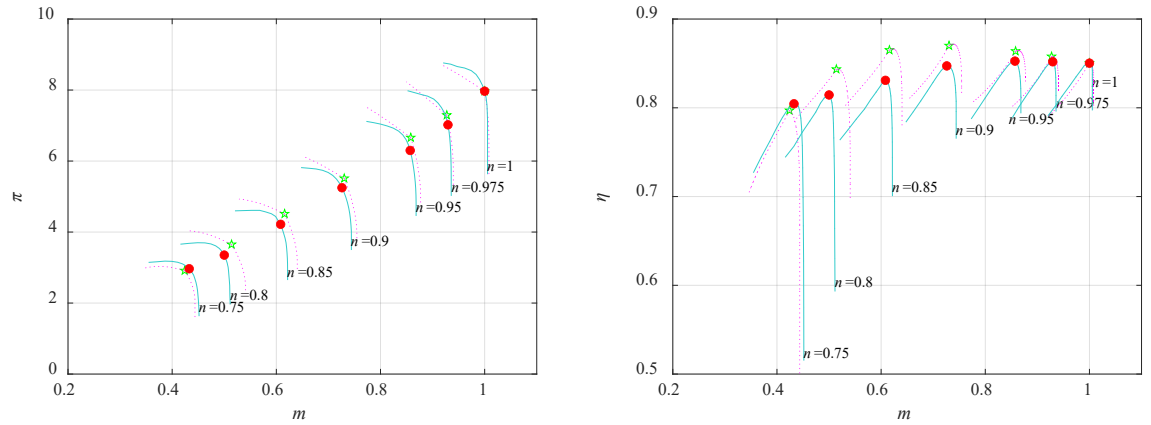

(b) Characteristics prediction of a six stages compressor

Figure 12 Comparison of predicted maps and true original maps

(Red dots and green stars represent true peak efficiency points and predicted ones respectively and solid lines and dashed lines represented true characteristics lines and predicted ones respectively.)

Two examples of characteristics prediction results and the original performance maps are shown in Figure 12. Red dots and green stars represent true peak efficiency points and the predicted ones respectively and solid lines and dashed lines represented true characteristics lines and predicted ones respectively. It can be seen that the prediction of our algorithm corresponds with the ground truth nearly exactly. The predicted pressure ratios and efficiencies are slightly higher than the true values. This is because the nonlinearity hidden in the relationship between pressure ratio, specific work and speed causes inaccuracy in Eq. (8) and Eq. (9). For compressors with larger total pressure ratios, the nonlinearity or inaccuracy is more obvious. So, in this paper the largest pressure ratio of prediction is limited to less than 8. For single stage compressors such as fans or rotors, the prediction accuracy is much higher. For the sake of space, the prediction results are no given.

It should be noted that the characteristics prediction does not include the surge margin estimation which will be further investigated. The results shown above use the original surge and choke boundaries, It can be seen that the prediction lines are able to capture most characteristics of compressors and there are slightly differences with original ones which are that both total pressure ratio and efficiency are slightly higher than the true values when n=0.8~0.9 . The reason is that there are still some nonlinear in the relation between different quantities and the linear fitting cannot describe the relation completely, however, the nonlinear is not obvious for compressors whose design total pressure ratio is less than 8. It is worth mentioning that not all the compressors can be predicted so well because several ones do not obey the laws we found above very well and the prediction errors are large, however, the number of this kind of compressors is quite small.

7.CONCLUSIONS

We have explored the laws hidden in the compressors characteristics from three aspects which are peak efficiency points, near-choked zones and near-surged zones. An algorithm to predict the performance map just base on design indexes has been developed. Two examples of prediction show the algorithm can work well. It can be concluded that: In the peak efficiency line of a compressor, the mass flow, specific work and total pressure ratio exponentially related to the speed. For mass flow and total pressure ration, the exponential coefficients are related with design total pressure ratio, while for specific work the exponential coefficient is float around a fixing value. The three coefficients can describe the distinction of different compressors that share the same design indexes. In the near-choked zone, total pressure ratio can be used as an

independent variable to describe the rules of characteristic lines, while in near-surged zone, the mass flow is suitable to describe the laws of performance lines. The algorithm we developed can predict compressors performance map accurately within working speed range for compressors whose design ratio is less than 8. However, there are still some limitations. The nonlinear relations hidden in the characteristic map need to be further explored.

NOMENCLATURE

π	Total pressure ratio
η	Efficiency
m	Mass flow rate
n	Rotation speed
Δh^*	Specific work
T	Torque
c_p	Specific heat at constant pressure

Subscript

d	Design points
p	Peak efficiency points

ACKNOWLEDGMENTS

The authors gratefully acknowledge the support of the National Natural Science Foundation of China (No. 51790512) and the Stable Support Project of Aero Engine Corporation of China.

REFERENCES

Agrawal, R,. Yunis, M. (1981). A Generalized Mathematical Model to Estimate Gas Turbine Starting Characteristics. *Proceedings of the ASME 1981 International Gas Turbine Conference and Products Show*. Houston, USA. March 9–12, 1981. 81-GT-202.

Bayomi, N., Abdel-Maksoud, R., & Rezk, M. (2013). Centrifugal compressor map prediction and modification. *Journal of King Abdulaziz University Engineering Science*s, 24(24), 73-88.

Dixon, S., Hall, C. (2014). *Fluid mechanics and thermodynamics of turbomachinery*. 7th ed. UK: Butterworth-Heinemann.

Fei, J., Zhao, N., Shi, Y. et al. (2016). Compressor Performance Prediction Using a Novel Feed-Forward Neural Network Based on Gaussian Kernel Function. *Advances in Mechanical Engineering*, 8(1), pp. 1–14.

Kurzke, J. (1996). How To Get Component Maps For Aircraft Gas Turbine Performance Calculations. *Proceedings of the ASME 1996 International Gas Turbine and Aeroengine Congress and Exhibition*. Birmingham, UK. June 10–13, 1996. 96-GT-164.

Kurzke, J. (2005). How to Create a Performance Model of a Gas Turbine From a Limited Amount of Information. *Proceedings of the ASME Turbo Expo 2005: Power for Land, Sea, and Air*. Nevada, USA. June 6–9, 2005, GT2005-68536.

Kurzke, J. (2011). Correlations Hidden in Compressor Maps. *Proceedings of the ASME 2011 Turbo Expo: Turbine Technical Conference and Exposition.* British Columbia, Canada. June 6–10, 2011. GT2011-45519.

Li, X., Yang, C., Wang, Y., et al. (2018). Compressor Map Regression Modelling Based on Partial Least Squares. *Royal Society Open Science.* 5(8):172454, pp. 1-11

Mikhailov, A., Akhmedzyanov, D., Akhmetov, Y., et al. (2014). Joint Prediction of Aircraft Gas Turbine Engine Axial Flow Compressor Off-Design Performance and Surge Line Based on the Expanded Method of Generalized Functions. *Aircraft and Rocket Engine Theory.* 57(3), pp. 291-296.

Mikhailov, A., Mikhailova, A., Akhmedzyanov, D., (2016). New 1-D Method for the Prediction of Axial-Flow Compressors Off-Design Performance. *Procedia Engineering.* 150(06), pp. 155-160.

Tsoutsanis, E., Li, Y,. Pilidis, P,. et al. (2012a). Part-Load Performance Of Gas Turbines-Part I: A Novel Compressor Map Generation Approach Suitable For Adaptive Simulation. *Proceedings of the ASME 2012 Gas Turbine India Conference.* Maharashtra, India. Dec 1, 2012. GTINDIA2012-9580.

Tsoutsanis, E., Li, Y,. Pilidis, P,. et al. (2012b). Part-Load Performance of Gas Turbines-Part II: Multi-Point Adaptation with Compressor Map Generation and GA Optimization. *Proceedings of the ASME 2012 Gas Turbine India Conference.* Maharashtra, India. Dec 1, 2012. GTINDIA2012-9581.

Tsoutsanis, E. (2014). A Component Map Tuning Method for Performance Prediction and Diagnostics of Gas Turbine Compressors. *Applied Energy.* 135(15), pp. 572-585.

Ying, Y., Bo, S., Peng, S., et al. (2014). Study on the Regression Method of Compressor Map Based on Partial Least Squares Regression Modeling. P*roceedings of the ASME Turbo Expo 2014: Turbine Technical Conference and Exposition.* Düsseldorf, Germany. June 16–20, 2014. GT2014-25705.

Wang, Z., Wang, Y., Qiao,W., et al. (2006). Extrapolating component maps into the low speed and simulation of windmilling performance of turbofan engine. *Journal of Propulsion Technology*. 27(02), pp.146-149+181.

Zagorowska, M,. Thornhill, N. (2017) Compressor map approximation using Chebyshev polynomials. *25th Mediterranean Conference on Control and Automation (MED)*. July 3-6 2017, 17046364.